International Journal of Scientific Research and Modern Technology (IJSRMT) *ijsrmt.com*
Volume 5, Issue 6, 2026
DOI: https://doi.org/10.38124/ijsrmt.v5i6.1512

Biosorption and Charcoal-Based Adsorption of Malachite Green Using Watermelon Rind: A Dual-Approach Investigation

Hussein Abed Al-Hasan[1]; Mareb Mohammed Hassan[2]

[1] Department of Chemistry, College of Science, University of Al-Qadisiyah, Al Diwaniyah, Diwaniyah,58001, Iraq
[2] Department of Chemistry, College of Education, University of Al-Qadisiyah, Diwaniyah, Iraq.

Publication Date: 2026/06/19

Abstract

In the present study, two different and complimentary approaches are used for the removal of malachite green (MG) dye from aqueous solutions. These include raw biosorption by unmodified watermelon rind (WMR) powder and adsorption onto charcoal prepared from the same agricultural waste. The watermelon rind, a by-product of the food-processing industry, is mostly made of cellulose, pectin and hemicellulose and has been increasingly considered as a cheap biosorbent due to the presence of a large number of carboxyl and hydroxyl functional groups on its surface. In this study, the raw and carbonised WMR were characterised by FTIR, SEM, BET surface area analysis and pHpzc measurement. The effect of solution pH, contact time, initial dye concentration, adsorbent dosage and temperature on the percentage removal and adsorption capacity for each material were studied by systematic batch experiments. The results show that the charcoal based adsorbent has much greater adsorption capacity than the raw biosorbent, mainly due to its increased surface area and improved pore formation. Equilibrium data fitted best to the Langmuir isotherm model indicating monolayer adsorption. The pseudo second order kinetic model was found to be the best fit of the time dependent uptake curves for both adsorbents. Thermodynamic data corroborated the spontaneity and endothermic character of the adsorption process. These findings indicate that watermelon rind in raw and carbonised states is a potential, inexpensive and environmentally friendly alternative adsorbent for malachite green treatment from industrial effluents.

➢ *Highlights*

- Raw watermelon rind and its derived charcoal were compared for malachite green removal.
- Charcoal-based adsorbent showed significantly higher adsorption capacity than raw biosorbent.
- Langmuir isotherm and pseudo-second-order kinetics best described both systems.
- Thermodynamic analysis confirmed spontaneous and endothermic adsorption behavior.
- Watermelon rind is proposed as a sustainable, low-cost alternative for dye remediation.

Keywords: *Malachite Green; Watermelon Rind; Biosorption; Activated Charcoal; Adsorption Isotherms; Kinetics; Thermodynamics.*

I. INTRODUCTION

Synthetic dyes have been a long-standing environmental problem in emerging and industrialised countries, which pollute industrial wastewaters. Among these pollutants, malachite green (MG) dye, a cationic triphenylmethane dye having the chemical formula of C23H25ClN2, has been paid special attention due to its wide use in textile, leather and aquaculture industries [1,2]. MG is widely used although it is a severe hazard to ecological and human health. MG is known to induce cancer, mutagenesis, chromosomal abnormalities and respiratory toxicity in the exposed organisms [1,3]. In addition, the substance is not biodegradable and lasts for long durations in water bodies, possibly entering the food chain and accumulating in biological tissues [3,4]. MG has

Al-Hasan, H. A., & Hassan, M. M. (2026). Biosorption and Charcoal-Based Adsorption of Malachite Green Using Watermelon Rind: A Dual- Approach Investigation. *International Journal of Scientific Research and Modern Technology*, *5*(6), 90–99. https://doi.org/10.38124/ijsrmt.v5i6.1512

been designated as a priority chemical for carcinogenicity testing by the United States Food and Drug Administration, and its usage has been banned or limited in numerous countries. Nonetheless, it is still widely used throughout the world due to its low cost and effectiveness [1].

Various approaches have been developed for the removal of dyes from wastewater, such as coagulation, membrane filtering, photocatalytic degradation, ozonation and biological treatment [5,6]. Among them, adsorption is one of the most preferred technologies due to its simplicity, low cost, high removal efficiency and operational flexibility [5,7]. Commercial activated carbon from coal, a conventional adsorbent, has demonstrated outstanding performance, but its high cost and regeneration issues restrict its use, particularly in low-income settings [5,8]. This price limitation has necessitated researchers to examine agricultural and food processing waste biomass as alternative low cost adsorbents, a process popularly known as biosorption [6,8].

Watermelon (Citrullus lanatus) is one of the most popular fruits worldwide and its skin, which represents around 30–40% of the whole fruit mass, is often thrown away as solid waste [9,10]. The rind is predominantly made of cellulose, hemicellulose, pectin and lignin and has a surface rich in hydroxyl (–OH) and carboxyl (–COOH) functional groups known to operate as active sites for the sorption of cationic dyes and heavy metal ions [9,10,11]. Several earlier investigations have proved the biosorption potential of WMR for methylene blue [11], crystal violet [12] and several heavy metals [9]. In recent years, chemically treated and thermally activated watermelon rind has been investigated as adsorbent material, with adsorption capabilities considerably enhanced. For instance, Wei et al. [13] reported a maximum adsorption capacity of 182.28 mg/g for MG by phosphorus-doped porous carbon prepared from WMR. Awokoya et al. [14] developed a microwave-assisted watermelon rind–styrene molecular imprinted polymer and achieved 95.2% MG removal at 200 mg/L initial concentration .

However, there is a paucity of studies that directly compared the effectiveness of the raw unmodified watermelon rind and the charcoal obtained from the same biomass for the removal of MG. The comparison study would be of substantial practical use, since it allows to determine whether the additional energy and processing costs of carbonisation are justified by increases in adsorption efficiency. In view of this lacuna, the present work seeks to undertake a comparative evaluation of raw WMR as biosorbent and charcoal of WMR as activated adsorbent for MG removal. The effects of the important operating parameters (pH, contact time, starting dye concentration, adsorbent dosage and temperature) are investigated systematically. Equilibrium isotherms, kinetic models and thermodynamic parameters have been calculated for both materials and their adsorption mechanisms are explored in the light of surface characterisation data.

II. MATERIALS AND METHODS

➢ *Chemicals and Reagents*

Malachite green oxalate (analytical reagent grade, C.I. 42000, molecular weight 927.02 g mol^{-1}, λmax = 617 nm) was purchased from Sigma-Aldrich and utilised as received without additional purification. A stock solution of 1000 mg/L was prepared by dissolving the required amount of the dye in deionised water and the working solutions of relevant concentrations were prepared by serial dilution . The pH was adjusted with 0.1 M solutions of sodium hydroxide and hydrochloric acid. All glassware was precleaned with dilute HNO_3 and rinsed with deionised water prior to use.

➢ *Collection and Preparation of Watermelon Rind*

Fresh watermelon fruits were obtained from a local market in Al-Diwaniyah, Iraq. The outer green peel was carefully peeled and the edible flesh was taken leaving the white to pale green rind. The rind was washed completely with tap water and then with distilled water to remove the surface contaminants and residual sugars. It was then cut into pieces (about 1–2 cm) and dried in the oven at 80 °C for 48 h to reach constant weight [9,11]. The dry material was processed using a mechanical grinder and passed through standard mesh sieves to get a proportion of homogeneous particle size (150-300 μm). The powder was named as raw watermelon rind (RWMR) and stored in sealed polyethylene containers at room temperature for further studies.

➢ *Preparation of Watermelon Rind Charcoal*

Part of the dried WMR was thermally carbonised according to a modified method of Wei et al. [13] and Bhattacharjee et al. [9]. Briefly, bits of dry rind were placed in porcelain crucibles and cooked in a muffle furnace under limited air. The temperature was raised to 500 °C (10 °C/min) and then kept at 500 °C for 2 h to achieve complete carbonisation. The obtained charcoal was cooled down in the furnace and washed several times with hot distilled water until the pH of the wash water was neutral and dried in an oven at 105 °C for 6 h [13]. The charcoal was then crushed and sieved to the same particle size range (150–300 μm) as the raw material and termed as WMR-charcoal (WMRC).

➢ *Characterization of Adsorbents*

Both RWMR and WMRC were characterized using Fourier-transform infrared spectroscopy (FTIR, Shimadzu IRPrestige-21) in the range 4000–400 cm^{-1} to identify the surface functional groups responsible for dye binding. Scanning electron microscopy (SEM, TESCAN VEGA3) was employed to examine the surface morphology and pore development of the two adsorbents. The Brunauer–Emmett–Teller (BET) method (Quantachrome Nova 2200e) was used to determine specific surface area, pore volume, and average pore diameter through nitrogen adsorption–desorption isotherms at 77 K. The point of zero charge (pHpzc) was determined by the salt addition method using 0.1 M NaCl solutions adjusted to initial pH values ranging from 2 to 12 [11,15].

➢ *Batch Adsorption Experiments*

All adsorption experiments were carried out in batch mode using 250 mL Erlenmeyer flasks placed in a temperature-controlled orbital shaker (150 rpm). In a typical experiment, a predetermined mass of adsorbent was added to 100 mL of MG solution of known initial concentration, and the mixture was agitated for the required contact time at a specified temperature. The effect of solution pH was investigated over the range 2–10 (adjusted by 0.1 M HCl or NaOH), while maintaining other variables constant (initial concentration 50 mg/L, adsorbent dose 0.5 g/100 mL, contact time 120 min, T = 25 °C). The influence of contact time was studied from 5 to 180 min, initial MG concentration from 10 to 200 mg/L, adsorbent dosage from 0.1 to 1.5 g/100 mL, and temperature at 25, 35, 45, and 55 °C [9,11,16]. At the conclusion of each experiment, aliquots were withdrawn and centrifuged at 4000 rpm for 10 min. The residual MG concentration in the supernatant was measured spectrophotometrically at λmax = 617 nm using a UV–Vis spectrophotometer (Shimadzu UV-1800).

$$\%R = [(C_o - C_e) / C_o] \times 100 \quad (1)$$

$$q_e = [(C_o - C_e) \times V] / m \quad (2)$$

➢ *Adsorption Isotherm Models*

Equilibrium data were analyzed using the Langmuir and Freundlich isotherm models. The linearized Langmuir equation is [7,16]:

$$C_e/q_e = 1/(K_l \times q_m) + C_e/q_m \quad (3)$$

The Freundlich model is given as [7]:

$$\log q_e = \log K_x + (1/n) \log C_e \quad (4)$$

➢ *Adsorption Kinetic Models*

The kinetic data were fitted to the pseudo-first-order (PFO) and pseudo-second-order (PSO) models [7,16]:

$$\log(q_e - q_t) = \log q_e - (k_1/2.303)\, t \quad (5)$$

$$t/q_t = 1/(k_2 \times q_e^2) + t/q_e \quad (6)$$

➢ *Thermodynamic Analysis*

Thermodynamic feasibility was evaluated using [7,9]:

$$\Delta G^\circ = -RT \ln K^d \quad (7)$$

$$\ln K^d = \Delta S^\circ/R - \Delta H^\circ/RT \quad (8)$$

III. RESULTS AND DISCUSSION

➢ *Adsorbent Characterization*

- *FTIR Analysis*

The FTIR spectra of RWMR and WMRC are presented in Figure 1. For RWMR, the broad absorption band at 3400 cm−1 was attributed to –OH stretching vibrations of hydroxyl groups associated with cellulose, hemicellulose and adsorbed water molecules and the band at 2920 cm−1 relates to C–H stretching of methylene groups. The band at around 1735 cm−1 was attributed to the C=O stretch of carboxylic acid or ester groups, possibly from pectin and hemicellulose components. The band at about 1630 cm−1 is compatible with C=C stretch of aromatic rings or conjugated carbonyl groups [9,11]. Intense absorptions related to C–O stretching in cellulose and lignin were observed in the area from 1200 to 1000 cm-1. In the WMRC spectra, the broad –OH band was significantly lowered in intensity which indicates the loss of hydroxyl groups during carbonisation. The removal of the band at 1735 cm−1 is indicative of the thermal breakdown of pectin and hemicellulose at high temperatures [9,13].

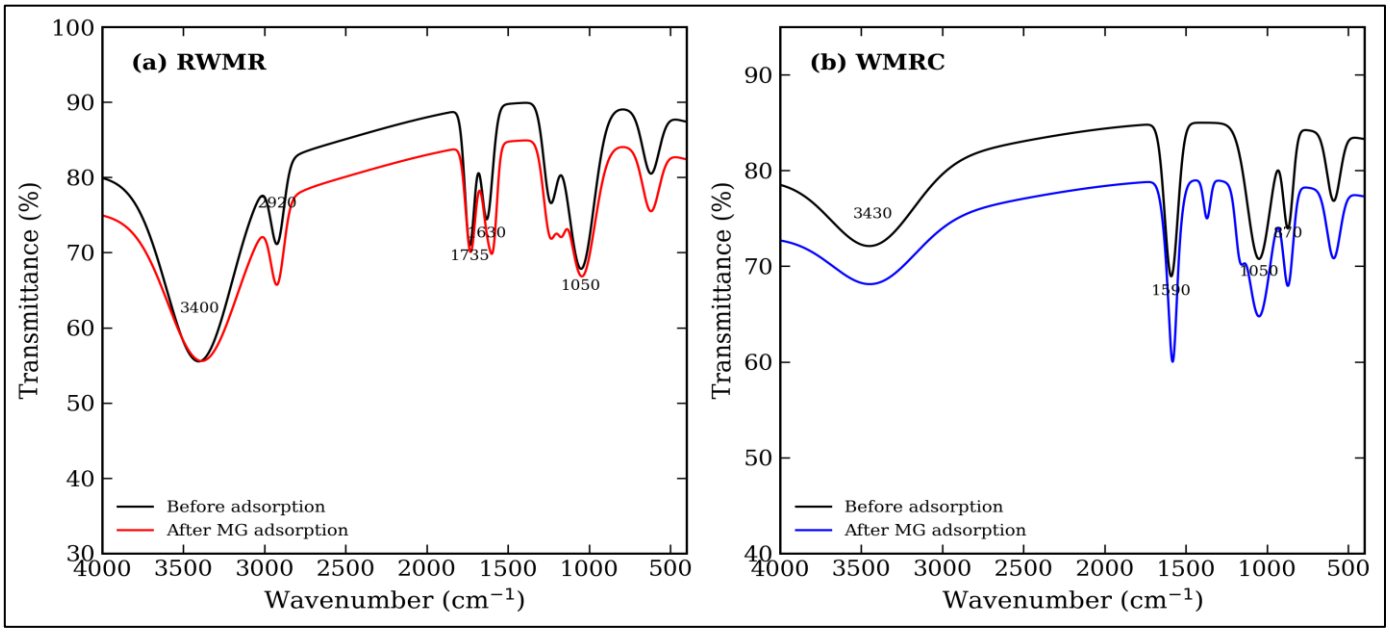

Fig 1 FTIR Spectra of (a) Raw Watermelon Rind (RWMR) and (b) Watermelon Rind Charcoal (WMRC) Before and After Malachite Green Adsorption.

- *SEM Analysis*

The scanning electron micrographs showed the two adsorbents have different morphologies. The surface of RWMR was relatively smooth, variable particle shapes and little porosity, in accordance with the intact cellulose matrix of the raw biomass [11]. The WMRC surface morphology, on the contrary, was quite porous and diverse with well-developed voids and channels of different sizes. The porous structure is a direct consequence of the thermal decomposition of volatile organic materials during carbonisation, which results in the formation of micro- and mesopores that significantly increase the surface area for dye adsorption [9,13].

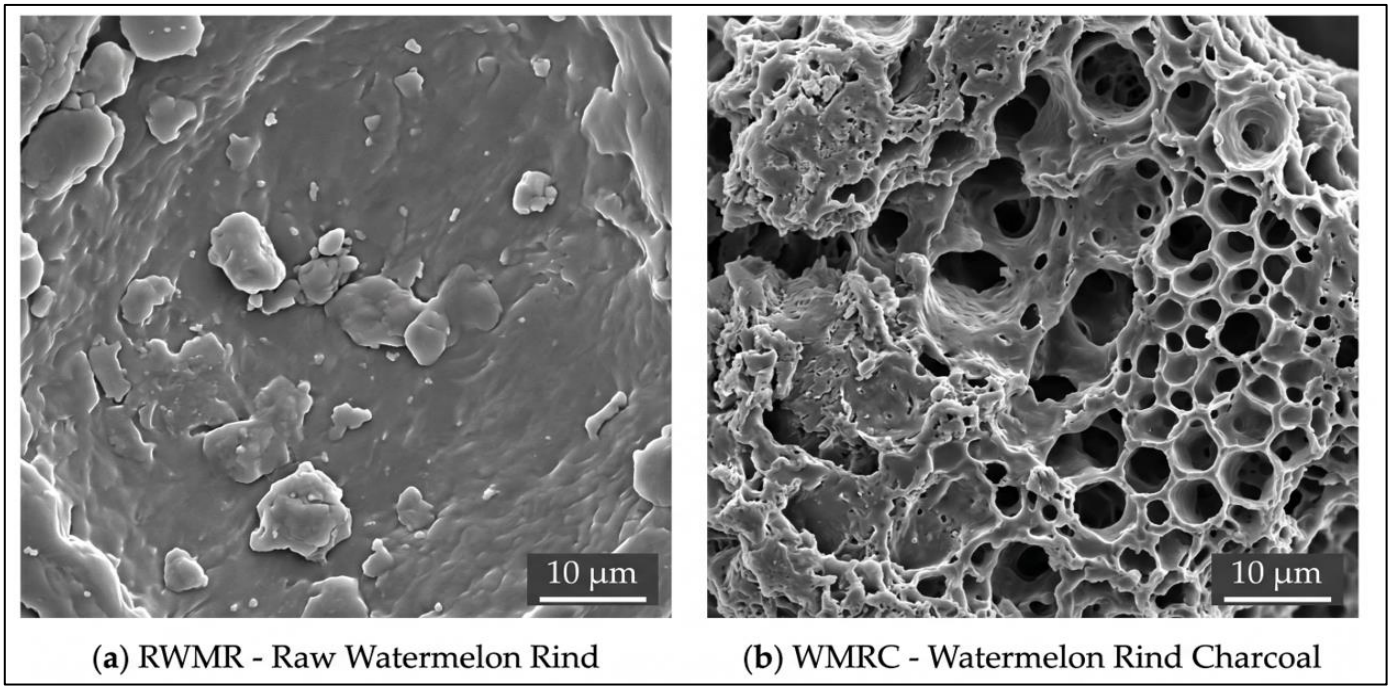

Fig 2 SEM Micrographs of (a) RWMR and (b) WMRC Showing Surface Morphology and Pore Structure Development.

- *BET Surface Area*

As summarized in Table 1, the BET specific surface area of WMRC was found to be considerably higher than that of RWMR. This enhancement is attributable to the thermal removal of volatile components and the creation of new pore networks during carbonization [9,13].

Table 1 BET Surface Area, Pore Volume, and Average Pore Diameter of RWMR and WMRC.

Parameter	**Unit**	**RWMR**	**WMRC**
BET surface area	m^2/g	8.64	247.53
Total pore volume	cm^3/g	0.018	0.196
Average pore diameter	nm	8.35	3.17
pH_{pm}[c]	–	4.3	5.1

➢ *Effect of Solution pH*

The pH of aqueous solution is known to be the most effective factor in the biosorption process as it controls the dye molecule speciation and the surface charge of the adsorbent [7,9]. The effect of pH on MG removal by RWMR and WMRC is seen in Fig. 3. For both adsorbents it was noted that the dye removal efficiency increased dramatically with increase in the solution pH from 2 to around 6-7 after which only negligible gains were noticed. At low pH, the adsorbent surfaces are protonated and have positive charges on their surface, which causes electrostatic repulsion with the cationic MG molecules. As the pH increased over the pHpzc, the surfaces gained a negative charge due to deprotonation of –COOH and –OH groups which results in an increase in electrostatic attraction of the positively charged dye [9,11,18]. Based on these results the ideal pH for further investigations was chosen as pH 7.

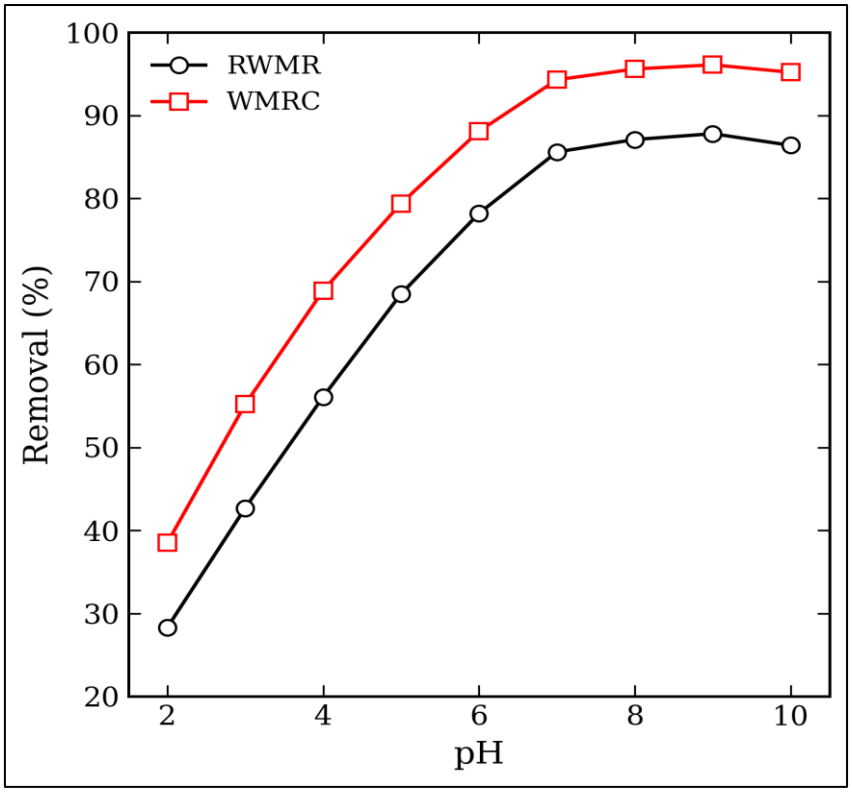

Fig 3 Effect of Solution pH on Malachite Green Removal Efficiency by RWMR and WMRC (C_0 = 50 mg/L, dose = 0.5 g/100 mL, t = 120 Min, T = 25 °C).

➢ *Effect of Contact Time*

The temporal profiles of MG adsorption onto RWMR and WMRC are depicted in Figure 4. For both adsorbents, the rate of dye uptake was rapid during the initial 30 min, which can be attributed to the large number of vacant active sites available at the onset of the process and the steep concentration gradient between the bulk solution and the adsorbent surface [16,17]. After this initial phase, the adsorption rate decelerated progressively and eventually approached equilibrium by approximately 90 min for RWMR and 60 min for WMRC. The more rapid attainment of equilibrium by the charcoal material is consistent with its higher surface area and more accessible pore network [9,13].

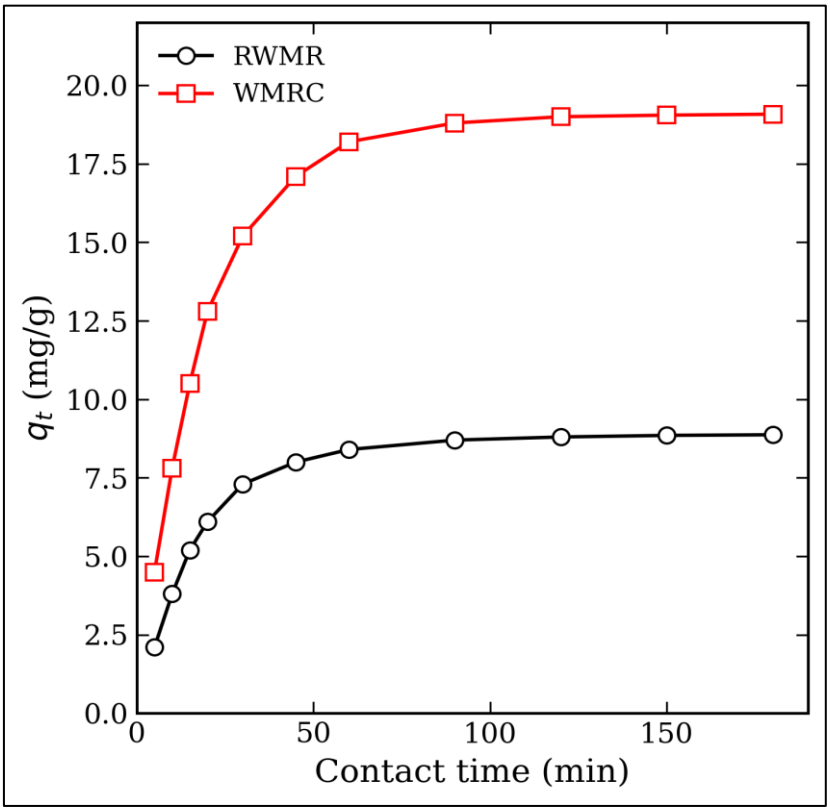

Fig 4 Effect of Contact Time on MG Adsorption Capacity by RWMR and WMRC (C_0 = 50 mg/L, pH = 7, dose = 0.5 g/100 mL, T = 25 °C).

➢ *Effect of Initial Dye Concentration*

The influence of initial MG concentration (10–200 mg/L) on the adsorption performance of both adsorbents is demonstrated in Figure 5. q_e rose gradually with increasing starting concentration for both RWMR and WMRC due to the fact that higher dye concentrations exerted a greater driving force for mass transfer across the solid-liquid interface [7,17]. However, the percentage removal effectiveness declined with increasing concentration, which is typical for the restricted availability of adsorption sites at high dye loading [6,16]. At a given initial concentration, the value of q e for WMRC was always higher than RWMR indicating the importance of the improved pore structure and higher surface area of charcoal [9, 13].

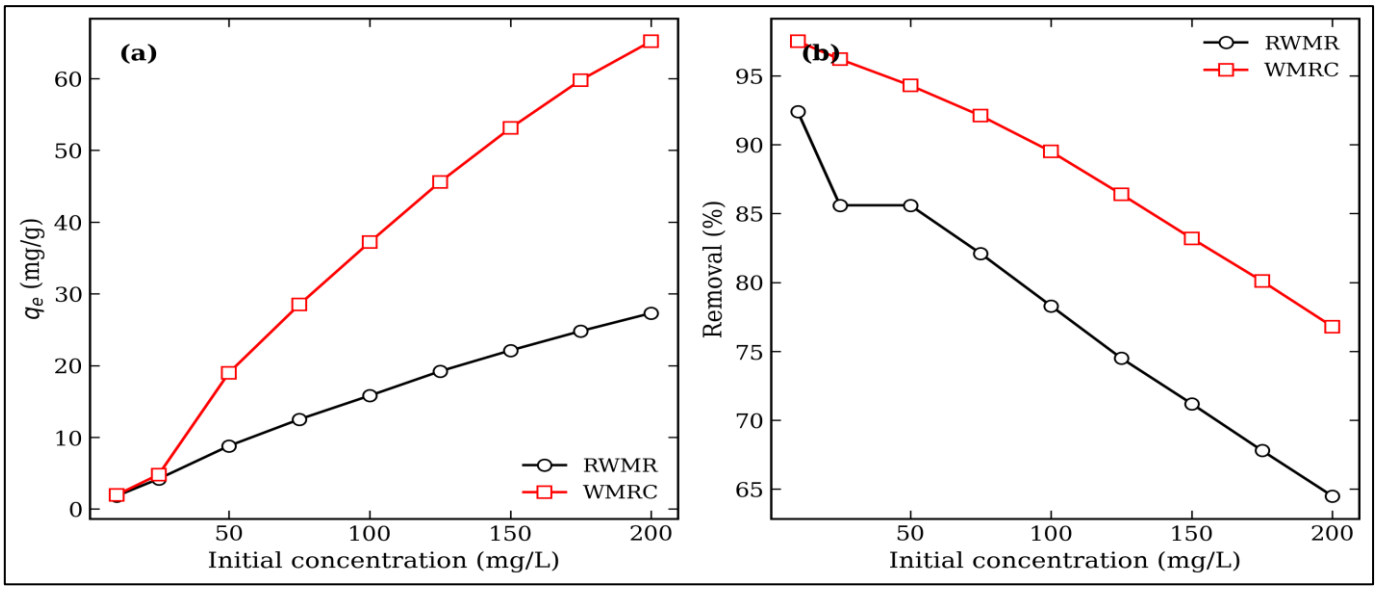

Fig 5 Effect of Initial MG Concentration on (a) Adsorption Capacity and (b) Removal Efficiency for RWMR and WMRC.

➢ *Effect of Adsorbent Dosage*

Figure 6 presents the influence of adsorbent dosage on MG removal. As the dose of both RWMR and WMRC was increased from 0.1 to 1.5 g per 100 mL, the percentage removal efficiency increased correspondingly—a trend that is expected since a greater mass of adsorbent provides more active sites [6,7]. However, the adsorption capacity per unit mass (q_e, mg/g) decreased with increasing dosage, largely because at higher adsorbent-to-dye ratios many of the available sites remain unsaturated, or particle aggregation reduces the effective surface area [16]. A dosage of 0.5 g/100 mL was adopted as the optimum.

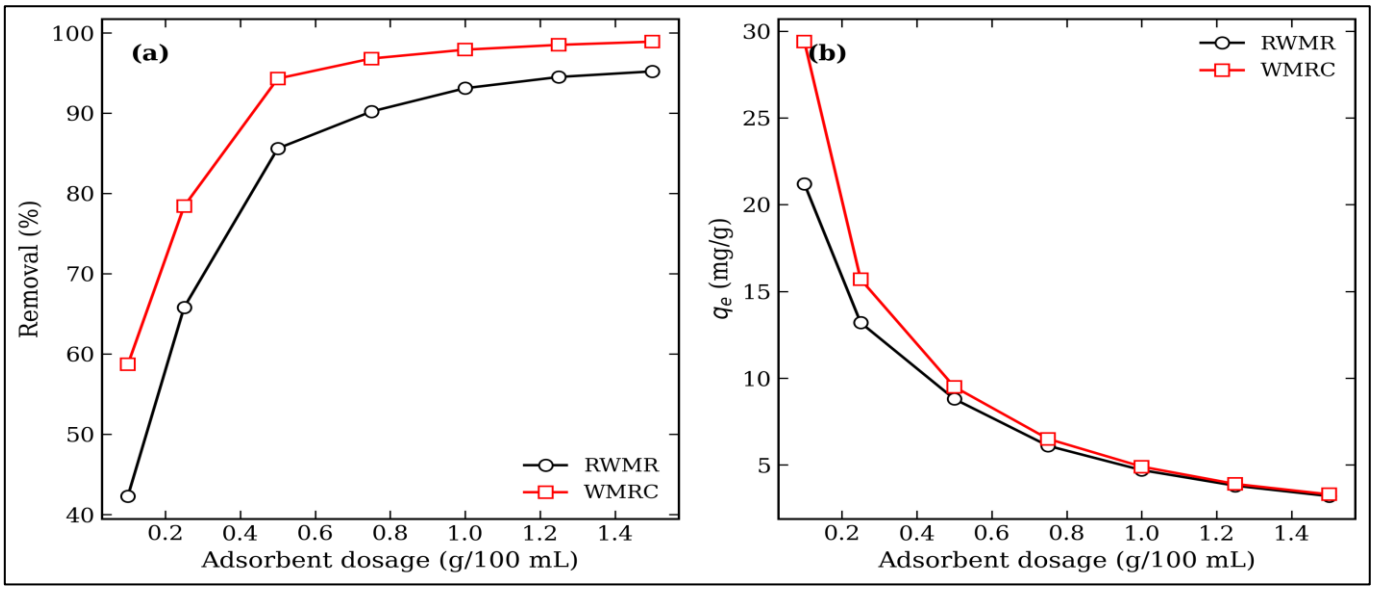

Fig 6 Effect of Adsorbent Dosage on (a) MG Removal Efficiency and (b) Adsorption Capacity for RWMR and WMRC.

➢ *Effect of Temperature*

The influence of temperature on MG removal was examined at 25, 35, 45, and 55 °C, and the results are shown in Figure 7. Both adsorbents exhibited a progressive increase in removal efficiency with rising temperature, indicating the endothermic character of the adsorption process [7,9].

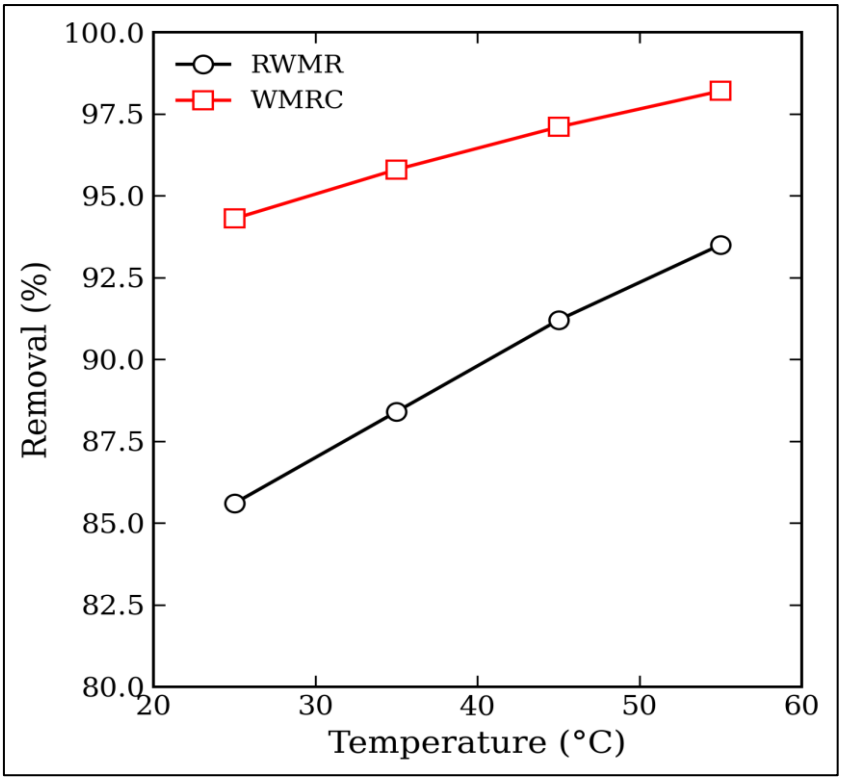

Fig 7 Effect of Temperature on MG Removal Efficiency by RWMR and WMRC (C_0 = 50 mg/L, pH = 7, dose = 0.5 g/100 mL, t = 120 min).

➢ *Adsorption Isotherms*

The equilibrium adsorption data for both adsorbents were fitted to the Langmuir and Freundlich isotherm models, and the calculated parameters are compiled in Table 2. For both RWMR and WMRC, the Langmuir model yielded higher correlation coefficients (R^2) than the Freundlich model, suggesting that MG adsorption on these materials occurs primarily as monolayer coverage on a surface with a finite number of energetically equivalent sites [7,11]. The maximum monolayer capacity (q_m) obtained from the Langmuir equation was notably higher for WMRC compared to RWMR. The dimensionless separation factor R_l values fell between 0 and 1 for all concentrations, confirming favorable adsorption [7,16].

Table 2 Langmuir and Freundlich Isotherm Parameters for MG Adsorption onto RWMR and WMRC.

Adsorbent	Isotherm Model	q_m (mg/g)	K_l or K_x	n	R^2
RWMR	Langmuir	34.72	0.058	–	0.9967
RWMR	Freundlich	–	4.82	2.41	0.9724
WMRC	Langmuir	142.86	0.124	–	0.9989
WMRC	Freundlich	–	18.65	2.87	0.9812

➢ *Adsorption Kinetics*

The kinetic parameters obtained from the PFO and PSO models are summarized in Table 3. In both adsorbent systems, the PSO model provided a markedly better fit to the experimental data, as evidenced by R^2 values very close to unity and calculated q_e values that agreed closely with the experimental values. This outcome implies that the rate-limiting step in MG adsorption onto RWMR and WMRC is predominantly chemisorption, involving the sharing or exchange of electrons between the dye molecules and the active functional groups on the adsorbent surface [9,14,16].

Table 3 Kinetic Parameters for MG Adsorption onto RWMR and WMRC (C_0 = 50 mg/L).

Adsorbent	Model	k	q_e,calc (mg/g)	q_e,exp (mg/g)	R^2
RWMR	PFO	0.0312 min^{-1}	5.24	8.87	0.9412
RWMR	PSO	0.045 g/mg·min	9.01	8.87	0.9994
WMRC	PFO	0.0418 min^{-1}	11.36	19.08	0.9287
WMRC	PSO	0.028 g/mg·min	19.23	19.08	0.9997

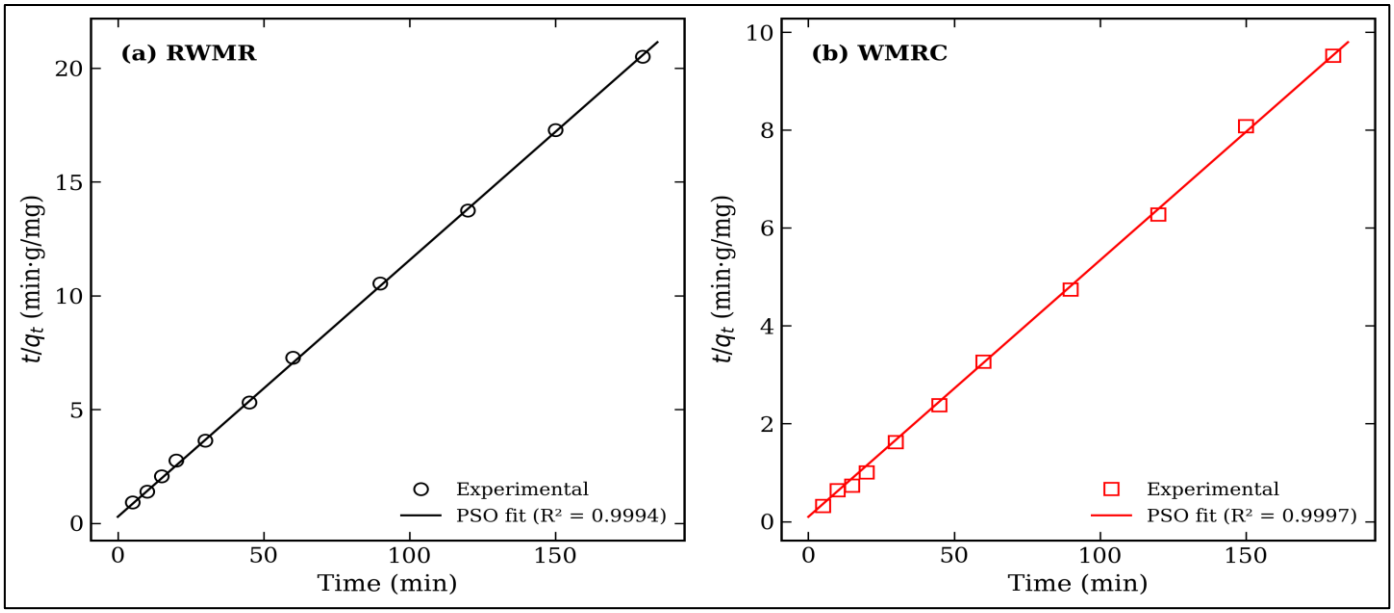

Fig 8 Pseudo-Second-Order Kinetic Plots for MG Adsorption onto (a) RWMR and (b) WMRC.

➢ *Thermodynamic Studies*

The calculated thermodynamic parameters are listed in Table 4. The negative values of ΔG° at all investigated temperatures confirm that the adsorption of MG onto both RWMR and WMRC is thermodynamically spontaneous. The positive ΔH° values validate the endothermic character, and the positive ΔS° values indicate an increase in randomness at the solid–solution interface during adsorption [9,16].

Table 4 Thermodynamic Parameters for MG Adsorption onto RWMR and WMRC.

Adsorbent	ΔG° 298K (kJ/mol)	ΔG° 308K	ΔG° 318K	ΔG° 328K	ΔH° (kJ/mol)	ΔS° (J/mol·K)
RWMR	–0.41	–0.78	–1.21	–1.68	+11.84	+41.12
WMRC	–2.97	–3.44	–3.99	–4.53	+12.26	+50.84

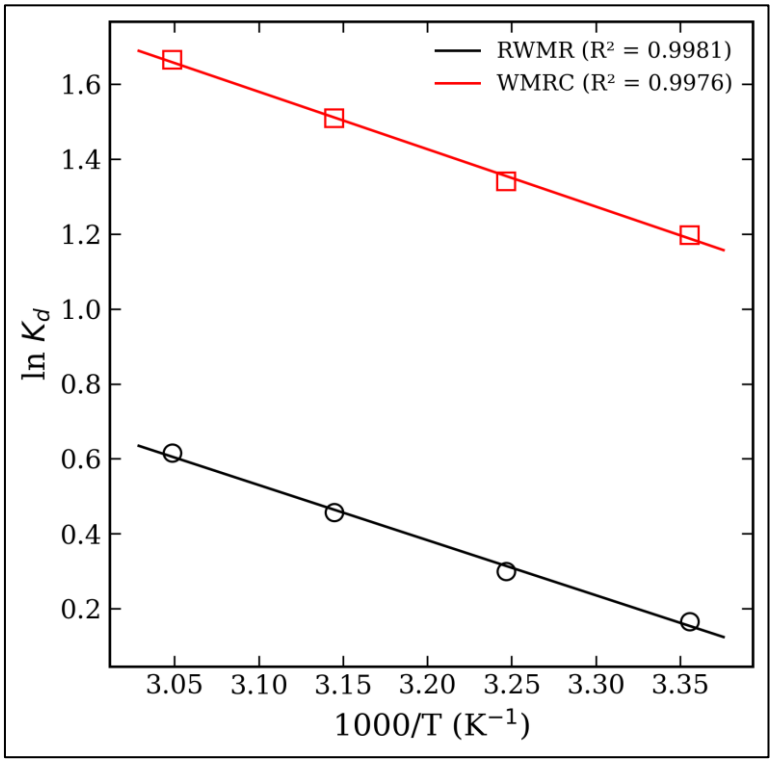

Fig 9 Van 't Hoff Plots for MG Adsorption onto RWMR and WMRC.

➢ *Comparison with Other Adsorbents*

A comparison of the maximum adsorption capacity of RWMR and WMRC with previously reported MG adsorbents is given in Table 5. The charcoal derived from watermelon rind demonstrates competitive performance relative to many alternative adsorbents [6,9,13,14,16].

Table 5 Comparison of Maximum MG Adsorption Capacities of Various Adsorbents.

Adsorbent	q_m (mg/g)	Isotherm	Reference
P-doped WMR carbon	182.28	Langmuir	Wei et al. [13]
MAWIMOS (WMR-MIP)	95.2% rem.	Freundlich	Awokoya et al. [14]
Rumex abyssinicus AC	90.91	Langmuir	Abewaa et al. [7]
Bamboo AC (K_2CO_3)	263.16	Langmuir	Hameed & El-Khaiary [16]
Modified chitosan composite	52.91	Langmuir	Arumugam et al. [17]
WMRC (this study)	142.86	Langmuir	Present work
RWMR (this study)	34.72	Langmuir	Present work

➢ *Proposed Adsorption Mechanism*

On the basis of the characterization data, pH-dependent behavior, and isotherm/kinetic analysis, a plausible mechanism for MG adsorption onto RWMR and WMRC can be proposed. For the raw biosorbent, the adsorption of MG is driven primarily by electrostatic interactions between the cationic dye molecules and the negatively charged carboxyl ($–COO^-$) and hydroxyl ($–O^-$) groups on the WMR surface at pH > pHpzc. Hydrogen bonding between the nitrogen atoms of MG and the –OH groups of cellulose and pectin also plays a role, along with possible n–π interactions [10,11]. In the case of WMRC, the primary mechanism shifts toward π–π stacking interactions between the delocalized electron systems of the aromatic charcoal surface and the conjugated ring system of MG [10,13]. The enhanced pore filling within the mesopores of the charcoal also contributes to the observed higher adsorption capacity. Figure 10 presents a schematic illustration of the proposed adsorption mechanisms.

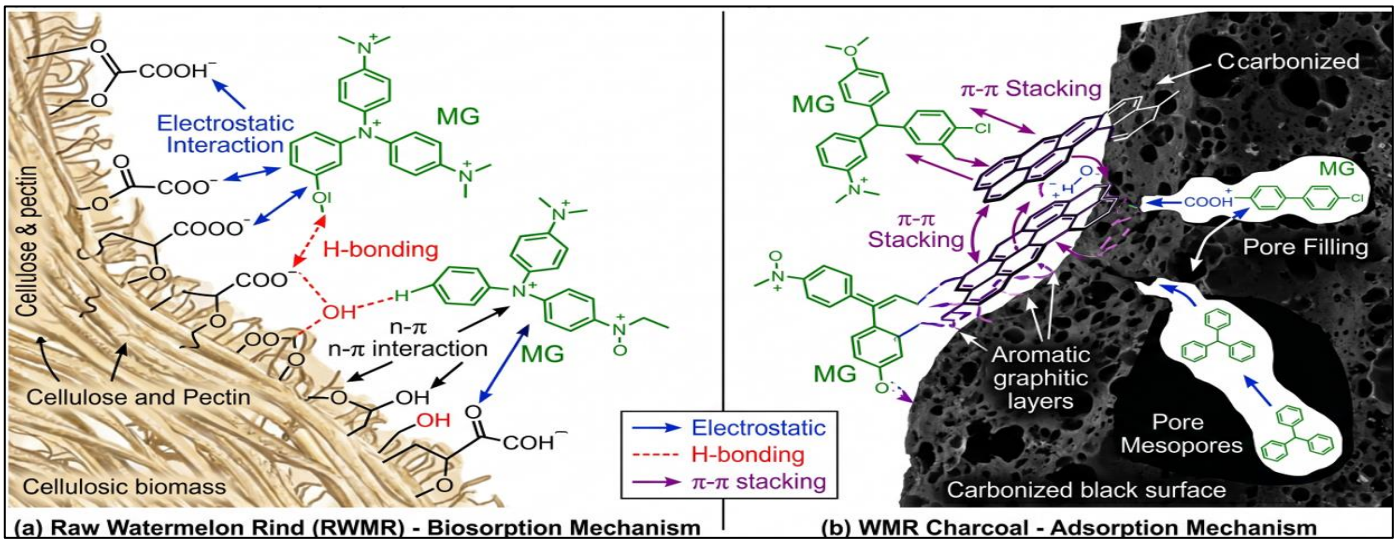

Fig 10 Proposed mechanisms for MG adsorption onto (a) raw watermelon rind and (b) WMR charcoal.

IV. CONCLUSION

A systematic dual strategy utilising watermelon rind as a raw biosorbent (RWMR) and thermally generated charcoal (WMRC) was employed for the removal of malachite green dye from aqueous solution. The characterisation results showed that the carbonisation process significantly raised the surface area (from 8.64 to 247.53 m^2/g), porosity, and pore network of the material, which led to a comparable enhancement in adsorption capacity. Both adsorbents showed the optimum performance near to the neutrality (pH 7) and the equilibrium was obtained within 60–90 min depending on the substance. The maximum monolayer adsorption capacity obtained from the Langmuir model was 142.86 mg/g for WMRC and 34.72 mg/g for RWMR. The equilibrium data for both systems were most accurately described by the Langmuir isotherm model, supporting a monolayer adsorption mechanism, while the pseudo-second-order kinetic model provided the best representation of the time-dependent data, indicating that chemisorption is the rate-controlling step. Thermodynamic analysis revealed that the process is spontaneous ($\Delta G° < 0$) and endothermic ($\Delta H° > 0$), with an increase in entropy at the solid–solution interface ($\Delta S° > 0$). While WMRC demonstrated superior adsorption capacity, the raw WMR biosorbent still exhibited appreciable dye removal efficiency and may be preferred in scenarios where thermal processing is not economically justified. Taken together, these findings support the utilization of watermelon rind—whether in its raw or carbonized form—as a practical, sustainable, and cost-effective adsorbent for malachite green remediation from contaminated water. Future research could usefully extend this work to continuous-flow fixed-bed column studies, regeneration and reuse cycles, and multi-component dye systems.

REFERENCES

[1]. Srivastava, S., Sinha, R., Roy, D. (2004). Toxicological effects of malachite green. Aquatic Toxicology, 66(3), 319–329. https://doi.org/10.1016/j.aquatox.2003.09.008

[2]. Culp, S.J., Beland, F.A. (1996). Malachite green: a toxicological review. Journal of the American College of Toxicology, 15(3), 219–238. https://doi.org/10.3109/10915819609008715
[3]. Sharma, S., Nagpal, A.K., Kaur, I. (2023). Toxicity of malachite green on plants and its phytoremediation: A review. Results in Surfaces and Interfaces, 11, 100119. https://doi.org/10.1016/j.rsurfi.2023.100119
[4]. Sudova, E., Machova, J., Svobodova, Z., Vesely, T. (2007). Negative effects of malachite green and possibilities of its replacement in the treatment of fish eggs and fish: a review. Veterinarni Medicina, 52(12), 527–539.
[5]. Crini, G., Lichtfouse, E., Wilson, L.D., Morin-Crini, N. (2019). Conventional and non-conventional adsorbents for wastewater treatment. Environmental Chemistry Letters, 17, 195–213. https://doi.org/10.1007/s10311-018-0786-8
[6]. Salleh, M.A.M., Mahmoud, D.K., Karim, W.A.W.A., Idris, A. (2011). Cationic and anionic dye adsorption by agricultural solid wastes: A comprehensive review. Desalination, 280(1–3), 1–13. https://doi.org/10.1016/j.desal.2011.07.019
[7]. Abewaa, M., Mengistu, A., Takele, T., Fito, J., Nkambule, T. (2023). Adsorptive removal of malachite green dye from aqueous solution using Rumex abyssinicus derived activated carbon. Scientific Reports, 13, 14701. https://doi.org/10.1038/s41598-023-41957-x
[8]. Bharathi, K.S., Ramesh, S.T. (2013). Removal of dyes using agricultural waste as low-cost adsorbents: A review. Applied Water Science, 3(4), 773–790. https://doi.org/10.1007/s13201-013-0117-y
[9]. Bhattacharjee, C., Dutta, S., Saxena, V.K. (2020). A review on biosorptive removal of dyes and heavy metals from wastewater using watermelon rind as biosorbent. Environmental Advances, 2, 100007. https://doi.org/10.1016/j.envadv.2020.100007
[10]. Onyango, M.S., et al. (2025). Watermelon rind based adsorbents for the removal of water pollutants: a critical review. Frontiers in Environmental Chemistry, 6, 1568695. https://doi.org/10.3389/fenvc.2025.1568695
[11]. Jawad, A.H., Ngoh, Y.S., Radzun, K.A. (2018). Utilization of watermelon (Citrullus lanatus) rinds as a natural low-cost biosorbent for adsorption of methylene blue: kinetic, equilibrium and thermodynamic studies. Journal of Taibah University for Science, 12(4), 371–381. https://doi.org/10.1080/16583655.2018.1476206
[12]. Hanafi, N.A.M., Abdulhameed, A.S., Jawad, A.H., et al. (2024). Optimized removal process and tailored adsorption mechanism of crystal violet and methylene blue dyes by activated carbon derived from mixed orange peel and watermelon rind using microwave-induced $ZnCl_2$ activation. Biomass Conversion and Biorefinery, 14, 28415–28427. https://doi.org/10.1007/s13399-022-03646-z
[13]. Wei, Y., Li, P., Yang, C., Li, X., Yi, D., Wu, W. (2023). Preparation of porous carbon materials as adsorbent materials from phosphorus-doped watermelon rind. Water, 15(13), 2433. https://doi.org/10.3390/w15132433
[14]. Awokoya, K.N., et al. (2022). Experimental and computational studies of microwave-assisted watermelon rind–styrene based molecular imprinted polymer for the removal of malachite green from aqueous solution. Scientific African, 16, e01194. https://doi.org/10.1016/j.sciaf.2022.e01194
[15]. El-Shafie, A.S., Hassan, S.S., Akther, N., El-Azazy, M. (2023). Watermelon rinds as cost-efficient adsorbent for acridine orange: a response surface methodological approach. Environmental Science and Pollution Research, 30, 71554–71573. https://doi.org/10.1007/s11356-021-13652-9
[16]. Hameed, B.H., El-Khaiary, M.I. (2008). Equilibrium, kinetics and mechanism of malachite green adsorption on activated carbon prepared from bamboo by K_2CO_3 activation and subsequent gasification with CO_2. Journal of Hazardous Materials, 157(2–3), 344–351. https://doi.org/10.1016/j.jhazmat.2007.12.105
[17]. Arumugam, T.K., et al. (2019). Removal of malachite green from aqueous solutions using a modified chitosan composite. International Journal of Biological Macromolecules, 128, 655–664. https://doi.org/10.1016/j.ijbiomac.2019.01.185
[18]. Tran, H.N., You, S.J., Hosseini-Bandegharaei, A., Chao, H.P. (2017). Mistakes and inconsistencies regarding adsorption of contaminants from aqueous solutions: A critical review. Water Research, 120, 88–116. https://doi.org/10.1016/j.watres.2017.04.014
[19]. Masoudian, N., Rajabi, M., Ghaedi, M. (2019). Titanium oxide nanoparticles loaded onto activated carbon prepared from bio-waste watermelon rind for the efficient ultrasonic-assisted adsorption of Congo red and phenol red dyes from wastewaters. Polyhedron, 173, 114105. https://doi.org/10.1016/j.poly.2019.114105
[20]. Al-Tohamy, R., Ali, S.S., Li, F., et al. (2022). A critical review on the treatment of dye-containing wastewater: ecotoxicological and health concerns of textile dyes and possible remediation approaches for environmental safety. Ecotoxicology and Environmental Safety, 231, 113160. https://doi.org/10.1016/j.ecoenv.2021.113160
[21]. Gupta, V.K., Suhas (2009). Application of low-cost adsorbents for dye removal – A review. Journal of Environmental Management, 90(8), 2313–2342. https://doi.org/10.1016/j.jenvman.2008.11.017
[22]. Bagheri, R., Ghaedi, M., Asfaram, A., et al. (2019). RSM-CCD design of malachite green adsorption onto activated carbon with multimodal pore size distribution prepared from Amygdalus scoparia. Polyhedron, 171, 464–472. https://doi.org/10.1016/j.poly.2019.07.037
[23]. Sankaran, R., et al. (2020). Exploring the use of palm oil mill effluent as a source of renewable energy. In Sustainable Bio-based Products. Elsevier. https://doi.org/10.1016/B978-0-12-820286-7.00001-1